

ABSORPTION AND LUMINESCENCE IN $\text{Bi}_{1-x}\text{Sb}_x$ ALLOYS

T.R. MEHDIYEV, Kh.A. GASANOVA

*G.M. Abdullayev Institute of Physics of Azerbaijan NAS**131, H. Javid ave., Baku, AZ 1143*

The photoluminescence spectra of $\text{Bi}_{0.97}\text{Sb}_{0.03}$, $\text{Bi}_{0.88}\text{Sb}_{0.12}$, and $\text{Bi}_{0.85}\text{Sb}_{0.15}$ alloys are presented at a temperature of 300 K in the range from 250 nm to 650 nm of the spectrum. The analysis of the spectra is carried out by decomposition into Lorentz-Gaussian components. Photoluminescence spectra were studied on LS-55 spectrometer (Perkin-Elmer) with Monck-Gillieson monochromator at room temperature in the wavelength range 300–700 nm at excitation from radiation 150W xenon source: 237 nm (5.23 eV), 285 nm (4.35 eV), 298 nm (4.16eV), 337nm (3.678eV), 377nm (3.288eV), 423nm (2.93eV). The accuracy of setting the wavelength is ± 1.0 nm, the reproducibility of the setting of the wavelength is ± 0.5 nm. The investigations carried out now, show that most crystalline media containing bismuth have inherent broad (50-80 nm) bands (blue (with luminescence lifetime $\tau \approx 1-2$ μs) and red ($\tau \approx 5-12$ μs)) luminescence. Even in the case of single crystals with bismuth, wide absorption and luminescence bands were observed, which was associated with the electron-phonon interaction of an optical center that is unusual for rare-earth ions, in which optical electrons are screened from the external field of the ligands.

Keywords: absorption, luminescence, $\text{Bi}_{1-x}\text{Sb}_x$ alloys.

PACS: 71.20. Nr, 72.20.My, 72.20.Fr, 73.50.Jt

INTRODUCTION

In recent decades, bismuth-antimony alloys have attracted attention, not only as a class of some of the best materials for thermoelectricity and cooling in the cryogenic temperature range, but also by the possibilities of using, for example, to create highly efficient laser information systems. At present, optical amplifiers have already been created in the range of 1420-1460 nm with parameters meeting the conditions for their use in information communication systems, and the maximum power of bismuth laser has reached 20 W at an efficiency of up to 50%. A serious obstacle to the improvement of these systems is the lack of an adequate model of the IR bismuth active center. Note that none of the discussed theoretical models doesn't satisfy to the modern experimental data [1].

Bismuth-antimony solid solutions are also interesting because various groups of electronic levels change their energy depending on the composition of Bi and Sb semimetals. The nature of the overlapping bands leading to semimetal behavior for elementary Bi and Sb is different. The bands dramatically change energy depending on the composition, and at values of x from 0.07 to 0.23 a real semiconductor is observed [2]. In narrow-gap semiconductor compositions, the states of the valence and conduction bands can be inverted in energy and, accordingly, surface states change, and the basal plane 111 or 001 has threefold rotation symmetry and topological surface states intersecting the Fermi energy an odd number of times. The Fermi surface for electrons in surface states is rather complicated, however, the composition $\text{Bi}_{0.9}\text{Sb}_{0.1}$ is almost an ideal material for studying topological surface states.

Studies conducted to date have shown that most crystalline media containing bismuth have inherent broad (50-80 nm) bands (blue (with luminescence lifetime $\tau \approx 1-2$ μs) and red ($\tau \approx 5-12$ μs)) luminescence. Even in the case of single crystals with bismuth, wide absorption and luminescence bands were observed, which was associated with the electron-phonon

interaction of optical center that is unusual for rare-earth ions, in which optical electrons are screened from the external field of the ligands. The analysis of published works showed that most of them were devoted to the study of bismuth in ordered media, which are known to be convenient media for studying the features and structure of optical centers, of which various hypotheses were proposed.

EXPERIMENTAL PART

The photoluminescence spectra of the $\text{Bi}_{0.97}\text{Sb}_{0.03}$, $\text{Bi}_{0.88}\text{Sb}_{0.12}$, and $\text{Bi}_{0.85}\text{Sb}_{0.15}$ alloys at a temperature of 300 K in the range from 250 nm to 650 nm of the spectrum are shown in fig. 1 and 5. An analysis of the spectra by decomposition into Lorentz-Gaussian components is shown in fig. 2-4 and in table 1. Photoluminescence spectra were studied on LS-55 spectrometer (Perkin-Elmer) with a Monck-Gillieson monochromator at room temperature in the wavelength range 300–700 nm when excited from a 150-watt xenon source: 237 nm (5.23 eV), 285 nm (4.35 eV), 298 nm (4.16eV), 337nm (3.678eV), 377nm (3.288eV), 423nm (2.93eV). The accuracy of setting the wavelength is ± 1.0 nm, the reproducibility of the setting of the wavelength is ± 0.5 nm.

Comparison of experimentally obtained photoluminescence spectra for the $\text{Bi}_{0.97}\text{Sb}_{0.03}$, $\text{Bi}_{0.88}\text{Sb}_{0.12}$ and c. $\text{Bi}_{0.85}\text{Sb}_{0.15}$ alloys at the temperature 300 K in the range from 250 nm to 650 nm with theoretical calculations by pseudopotential method, in which the fitting of Bi and Sb pseudopotentials to the experimentally investigated optical absorption spectra [3], is given in table 1.

As indicated, a feature of bismuth-antimony solid solutions is the existence of various groups of electronic levels, the energies of which vary depending on the composition of the Bi and Sb semimetals, and a semimetal-semiconductor phase transition is observed at x values from 0.07 to 0.23 [2].

Note that the formation of spectral bands indicating a phase transition to semimetal behavior for

ABSORPTION AND LUMINESCENCE IN $\text{Bi}_{1-x}\text{Sb}_x$ ALLOYS

elementary Bi and Sb, and their compounds are different. As an example, experimental studies of materials containing bismuth showed that blue luminescence ($\approx 400\text{-}500\text{nm}$) arises as a result of the $^3\text{P}_1 \rightarrow ^1\text{S}_0$ electronic transition between the energy levels of the Bi^{3+} ion, while the appearance of red luminescence ($\approx 590\text{-}640\text{nm}$) is due to the transition $^2\text{P}_{3/2}(1) \rightarrow ^2\text{P}_{1/2}$, bound to the Bi^{2+} ion.

Similarly, the appearance of bright blue luminescence in the spectral region from 470 nm to 515 nm upon excitation of 280 nm in antimony materials was attributed to Sb^{3+} [4]. The Stokes shift of Sb^{3+} in the compound $\text{Ca}_{10}(\text{PO}_4)_6(\text{F},\text{Cl})$ reaches

19000 cm^{-1} , which is usually observed for other materials at low temperatures [5]. Comparison of the energies of electronic transitions obtained from experimental photoluminescence spectra for the $\text{Bi}_{0.97}\text{Sb}_{0.03}$, $\text{Bi}_{0.88}\text{Sb}_{0.12}$ and $\text{Bi}_{0.85}\text{Sb}_{0.15}$ alloys at a temperature of 300 K in the range from 250 nm to 650 nm (see table 1) and theoretical calculations of the band structure pseudopotential method, in which, in order to establish reliable energy spectra, we used the fitting of Bi and Sb pseudopotentials to experimentally studied optical absorption spectra [3,6], to a first approximation, showed good agreement between them.

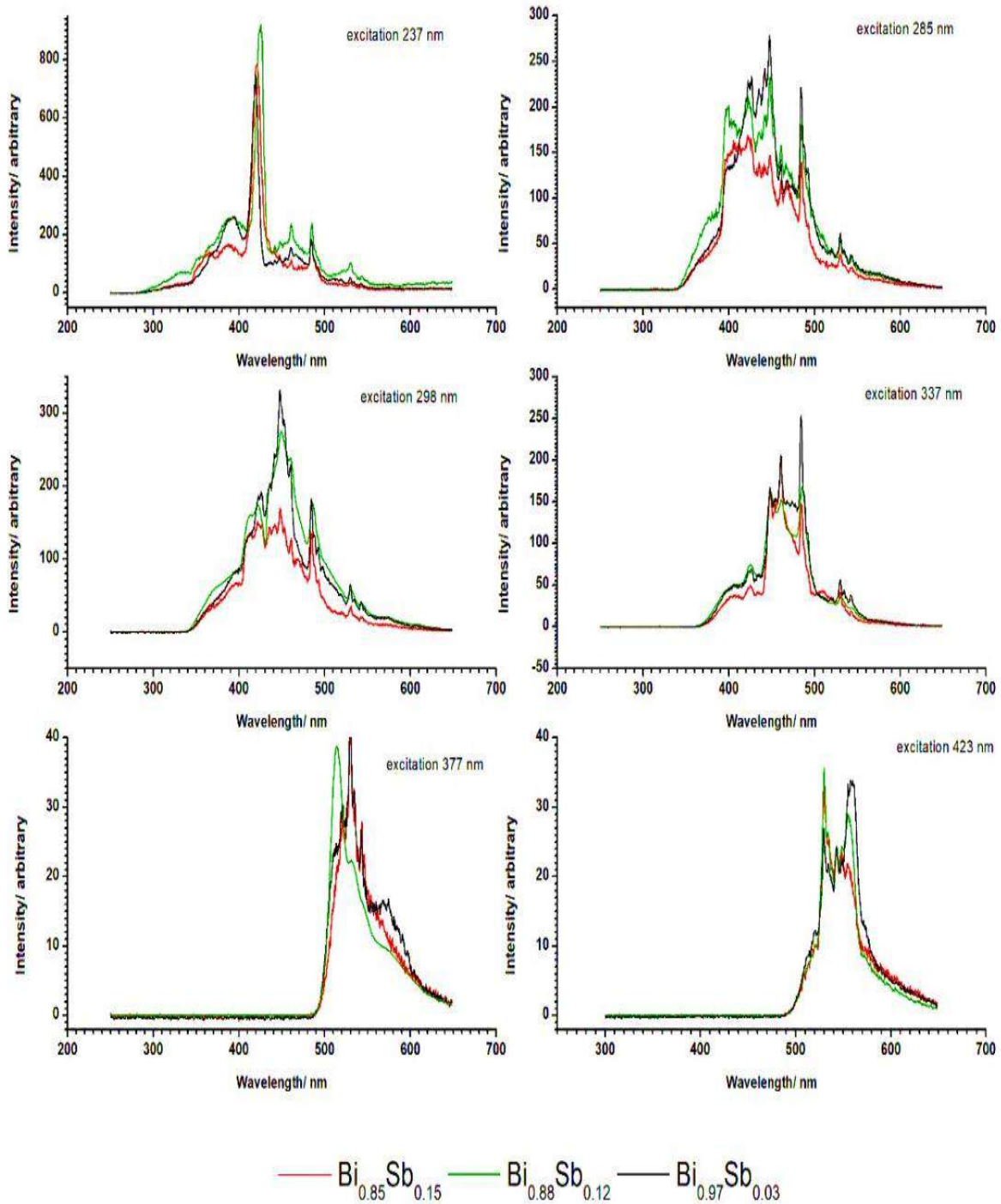


Fig. 1. Luminescence spectra of $\text{Bi}_{1-x}\text{Sb}_x$ alloys grouped by excitation lines.

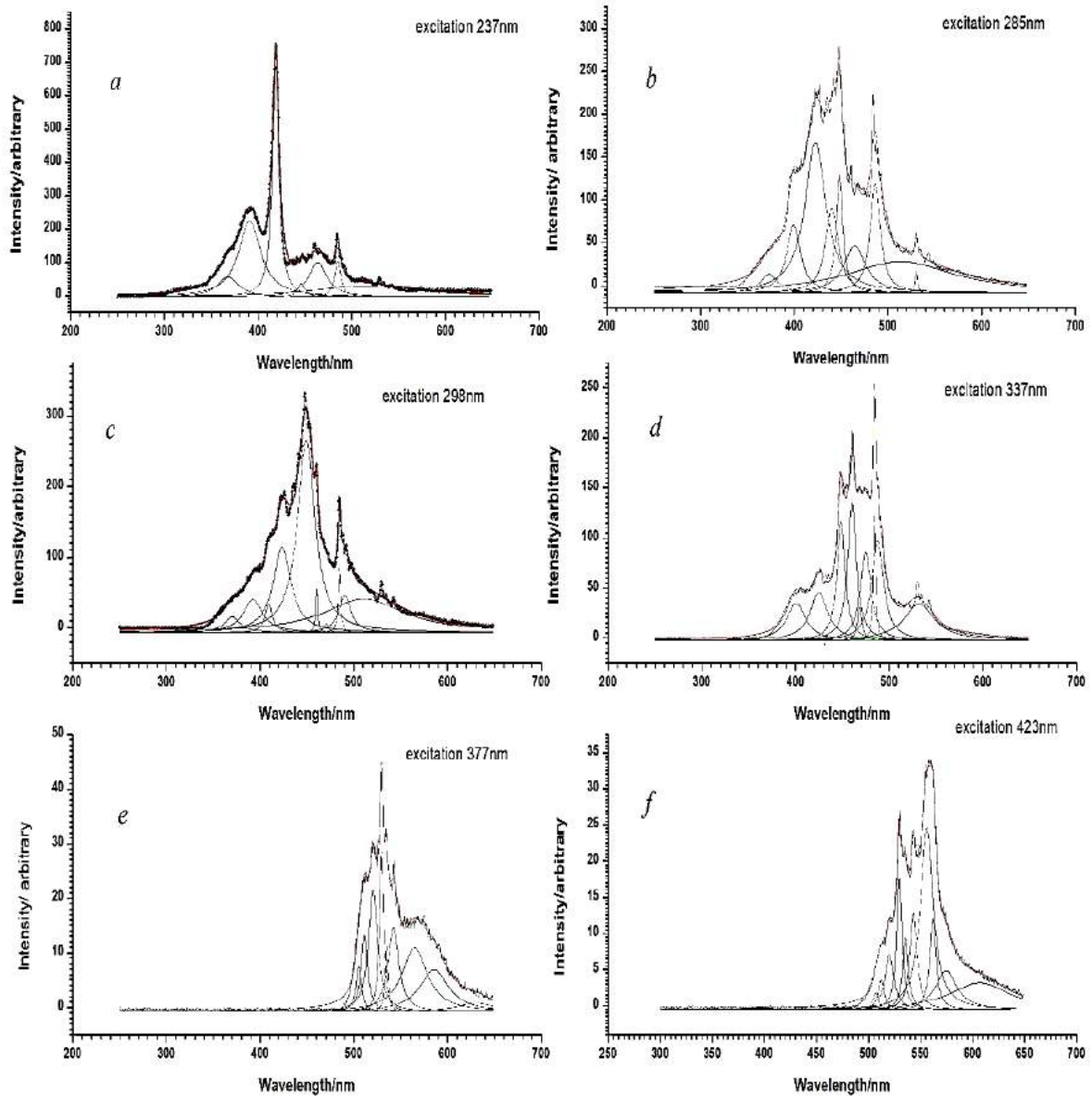


Fig.2. Decomposition of the luminescence spectra of $\text{Bi}_{0.97}\text{Sb}_{0.03}$ into Lorentz-Gaussian components (indicated in blue). The resulting spectrum is indicated in red.

In table 1, the luminescence maxima corresponding to pseudopotential calculations of the band structures of bismuth and antimony are highlighted in red. However, as one would expect, the photoluminescence spectra of $\text{Bi}_{0.97}\text{Sb}_{0.03}$, $\text{Bi}_{0.88}\text{Sb}_{0.12}$ and $\text{Bi}_{0.85}\text{Sb}_{0.15}$ have a more complex picture of transitions related by luminescence to the “blue” (400-500) nm and “red” (590-640) nm spectral bands, as well as their overlap. The observed pattern of electronic transitions is substantially complicated by the fact that bismuth and antimony are among the heavy p-elements, like Sn, Pb, and Tl, which in some of their compounds (for example, $\text{Bi}_{1-x}\text{Sb}_x$) have a valence of two units less than the group number. This phenomenon, called the

inert pair effect, is structurally observed in distortions of the coordination environment of metal ions. The trivalent Bi^{3+} and Sb^{3+} ions have electronic coordination $[\text{Xe}] 4f^{14}5d^{10}6s^2$ и $[\text{Kr}] 4d^{10}5s^2$, that is, the $6s_2$ pair becomes “stereo chemically active” due to the fact that it is not on the spherical orbital, it is asymmetrically displaced relative to the center of the ion (similar to what happens when the formation of hybridized sp -orbitals). As a result, various types of structure distortion may occur [7]. On the other hand, analysis of the data on the radii of antimony and bismuth ions can easily notice a large difference between them. [8].

ion	0	-1	-2	-3	-4	-5
Sb	0.161	0.114	0.095	0.082	0.075	0.062
Bi	0.182	0.148	0.117	0.102	0.086	0.075

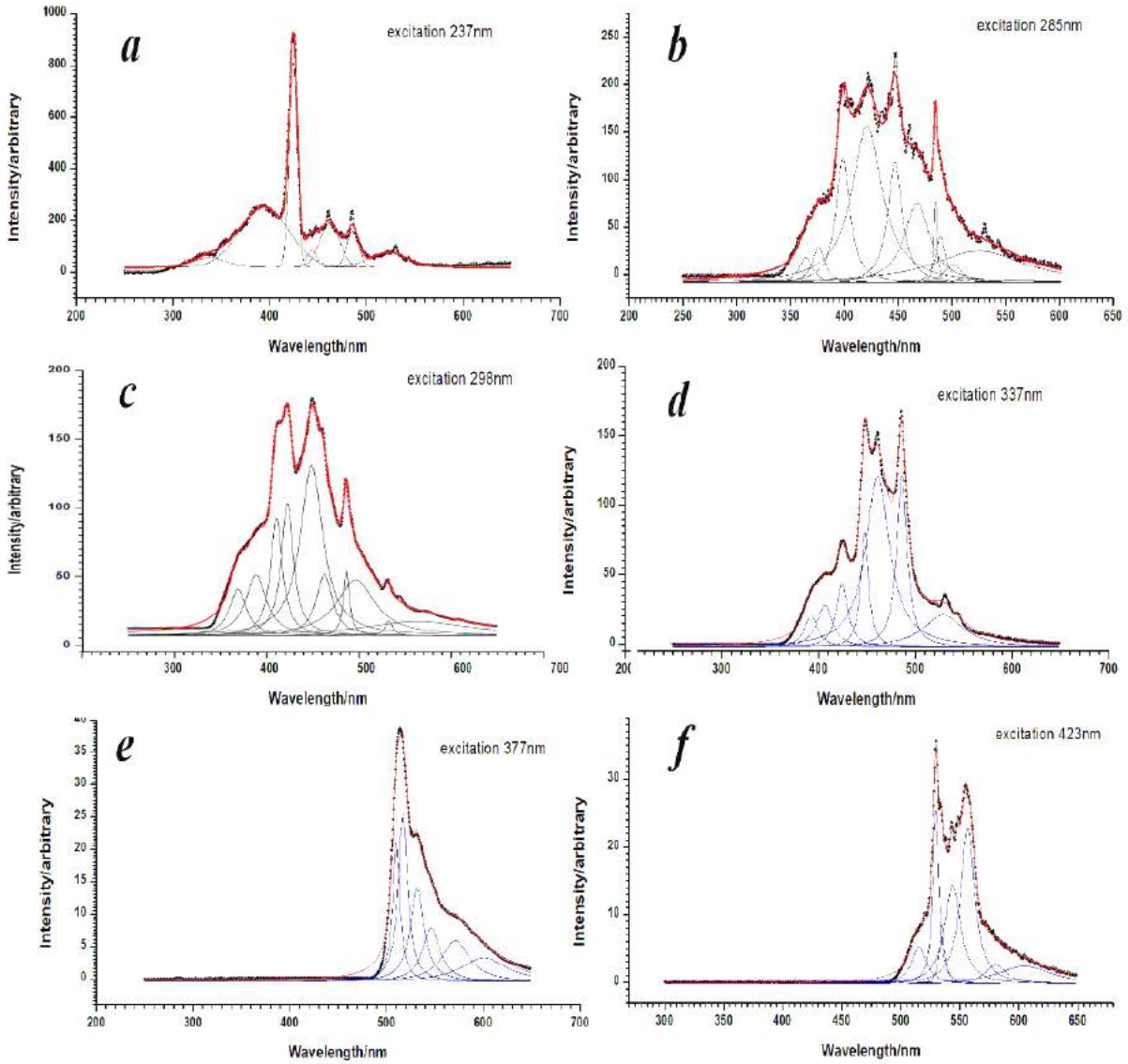
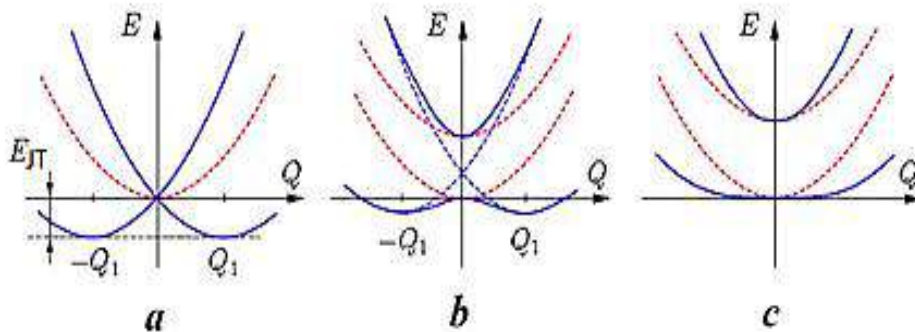


Fig.3. Decomposition of the luminescence spectra of $\text{Bi}_{0.88}\text{Sb}_{0.12}$ into Lorentz-Gaussian components.

As a result, arising geometric distortions of the structure of $\text{Bi}_{1-x}\text{Sb}_x$ compositions with respect to pure starting components should lead to a decrease in symmetry, splitting of degenerate states, i.e., to the Jahn-Teller effect, or the need to take into account vibronic interactions. Note that a complete classification of possible point groups of crystals subjected to Jahn-Teller strains is given in [9]. To describe the Jahn-

Teller (or vibronic) interactions of electrons with nuclei, they often resort to the formalism of potential energy surfaces. In the quadratic approximation, the potential energy surface corresponds to second-order hypersurface $E(Q)$, which is parameterized by the constants F_1 and K_1 and, in the one - dimensional case it degenerates to the parabolic curves shown schematically in figures (a, b, c) below.



The dashed line in the graph is the initial adiabatic potential for the highly symmetric undeformed nuclear configuration $Q=0$. Taking the Jahn-Teller effect into account leads to splitting of this curve into two components with minima at the points $Q_i=0$. In general, the number of intersecting branches of the adiabatic potential is equal to the degree of degeneracy electronic levels N . Thus, the minimum at the zero point disappears and new states $\pm Q_i$ appear, which correspond to low-symmetric deformed system configurations. The statement of system instability in $Q=0$ is called the simple Jahn-Teller effect. However, phenomena similar to the Jahn-Teller effect can be observed in systems with quasi degeneracy [10,11]. By definition, in the presence of quasi degeneracy, the electronic levels are quite close, but do not coincide, which is depicted as being close to each other by disjoint potential curves (see fig. b, c). Taking into account the Jahn-Teller pseudo-effect leads to the fact that the initial system at the point $Q=0$ either softens (fig. c) or becomes unstable (fig. b). Note that almost all molecular systems are subject to PEJT, in contrast to the simple effect of JT, which strictly requires degeneration of levels.

Periodically located translation Jahn-Teller centers may be subject to the cooperative effect. With sufficient approximation of neighboring centers, the external molecular field of each ceases to be isotropic. The nonequivalence of the effects leads to the stabilization of one of the possible directions of deformation for each center. In this case, one can observe the structural phase transition from the state of crystal with dynamically disordered Jahn-Teller systems to the state with completely static centers. This type of vibronic interactions is called the cooperative Jan-Teller effect. The mentioned correlation of deformations can be destroyed by strong temperature vibrations of the lattice. The fracture temperature of an ordered system of static centers depends on the strength of Jahn-Teller effect in particular Jahn-Teller crystal. Note that, when this is important, it is important to take into account the environment of the ion, that is, the influence of the asymmetric components of the crystal field of the lattice as the effect of some external potential. Theoretically, this means that the imposition of a small external disturbance can stabilize the system in one of the low-symmetry states. In this case, the static Jan-Teller effect occurs. An external disturbance can also create additional Q_i distortions in the already deformed Jahn-Teller system (see the fig. a, b, c). If the forces of the external low-symmetric action are greater than the Jahn-Teller forces, then the Jahn-Teller effect can be completely suppressed. In crystals of anionic complexes, a complete removal of JT distortions can be expected where the Jahn-Teller ion is chemically modified, or there is a strong coordination bond of the ion with other components of the complex. In the case of small perturbations, the so-called vibronic amplification [10,12] can be observed, and the coefficient of vibronic amplifications completely depends on the elastic constants of the molecular framework and the perturbation force (for example, in Cu^2 , Mn^3 , etc., this coefficient reaches ≈ 40). In systems

with a small external influence, the forces of external perturbations can play a stabilizing role if they make the Jahn-Teller minima on the surface of potential energy nonequivalent and the system is at the deepest minimum. Thus, the redistribution of minima on the surface of potential energy should not be isotropic. On the contrary, a highly symmetric environment is not able to stabilize the deformations of the Jahn-Teller ion. In crystals, such nonequivalent interactions are transmitted through the van der Waals forces, hydrogen bonds, and the cooperative Jahn-Teller effect.

Figure 6 shows the excitation spectra of (a) and luminescence (b) of $\text{Bi}_{0.97}\text{Sb}_{0.03}$ (semi-metallic state). The maximum of the spectral line 257nm of the excitation spectrum, according to the principle of Levshin's mirror symmetry, corresponds to a maximum of 419nm luminescence, relative to the label 338nm. Inverted specularly relative to the label, the excitation spectrum (indicated in blue) is combined with the luminescence spectrum. If we assume that a maximum of 257nm (4.82eV) corresponds to the $^1S_0 \rightarrow ^1P_1$ transition in Bi^{3+} , then the $^3P_1 \rightarrow ^1S_0$, transition, corresponding in this case to the maximum of 419nm (2.96eV) of the luminescence spectrum, should, according to pseudopotential calculations of the bismuth band structure [6], occur on the line of symmetry $L_s \rightarrow L_a$. The observed Stokes shift is 261nm. However, we note that the $^3P_1 \rightarrow ^1S_0$ transition is observed not only in all $\text{Bi}_{1-x}\text{Sb}_x$ compositions, but also on the luminescence spectra upon excitations by 298 nm (4.16eV) and 337nm (3.678eV) radiation. The latter turns out to be explainable, since the luminescence spectrum of $\text{Bi}_{0.97}\text{Sb}_{0.03}$ shows similar but low-intensity structures, which are confirmed upon excitation at 285 nm (4.35eV), 298 nm (4.16eV) and 337 nm (3.678eV) (see fig. 5a). The sequence of their location from each other corresponds to: 190meV between 1-2 spectra; 80 meV between 2-3 spectra (or 270 meV between 1-3 spectra), which are close in value to the vibrational frequencies, and may well indicate the presence of cooperative PEJT, as well as indicated in [13], the Johns-Peierls transition. A similar structure is found in the $\text{Bi}_{1-x}\text{Sb}_x$ spectra under excitations of 377nm and 423nm (see figs. 1–5), and the luminescence spectra for all the studied compositions are outwardly similar. On the luminescence spectra of $\text{Bi}_{1-x}\text{Sb}_x$ (fig. 1), it is easy to see how the overlap of the luminescence spectra of Bi and Sb changes.

However, if the presence of “blue” luminescence in $\text{Bi}_{1-x}\text{Sb}_x$ was not in doubt, then the presence of a weak “red” is possible only when Bi or Sb are in divalent states. Of course, we can assume the existence of small concentrations of defective or impurity centers of divalent Bi^{2+} and Sb^{2+} ions, especially since, as can be seen from table 1, the corresponding transitions can be selected for this. However, the goal of these studies was only to detect the cooperative effect of PEAT in $\text{Bi}_{1-x}\text{Sb}_x$. Oddly enough, in scientific publications information on the luminescence associated with electronic transitions in the ultraviolet and visible spectral ranges of $\text{Bi}_{1-x}\text{Sb}_x$ alloys is practically absent. Table 1 shows all the electronic transitions experimentally detected in the luminescence spectra.

ABSORPTION AND LUMINESCENCE IN $\text{Bi}_{1-x}\text{Sb}_x$ ALLOYS

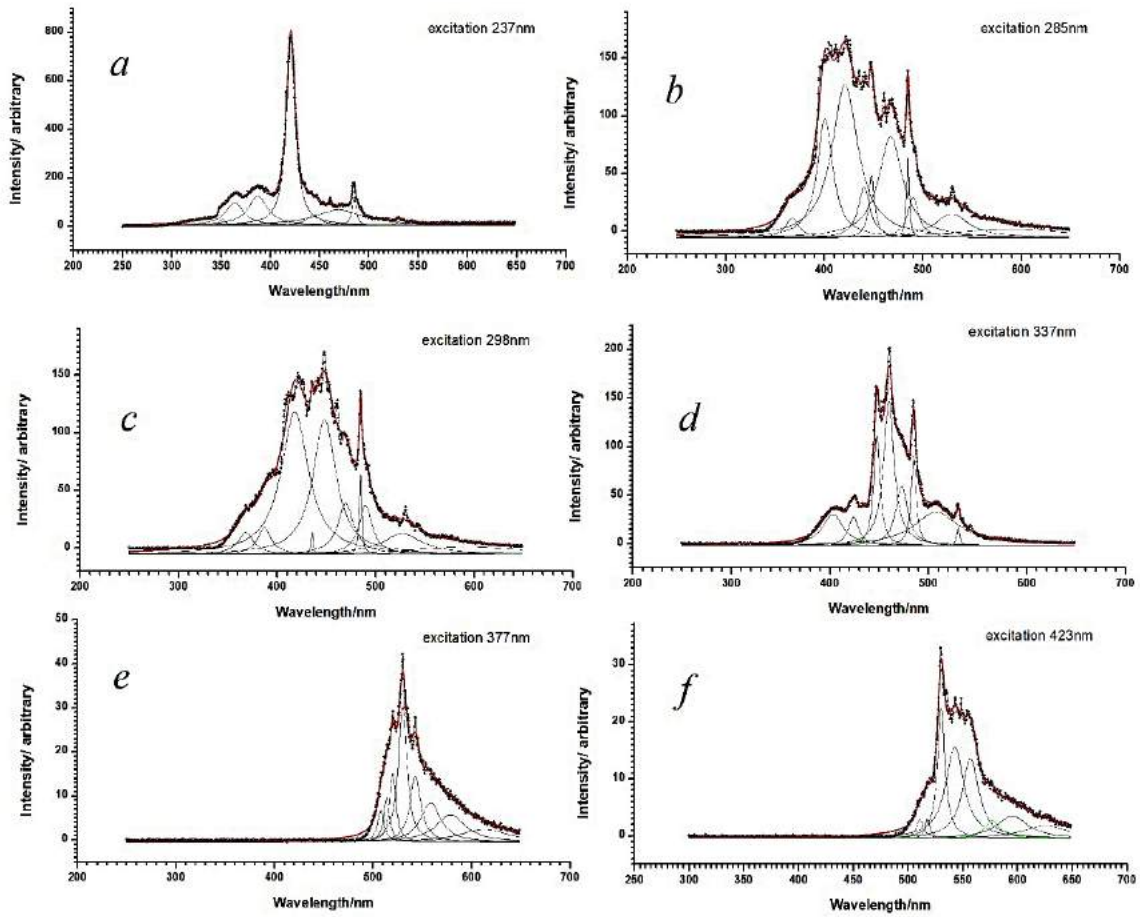


Fig. 4. Decomposition of the luminescence spectra of $\text{Bi}_{0.85}\text{Sb}_{0.15}$ into Lorentz-Gaussian components.

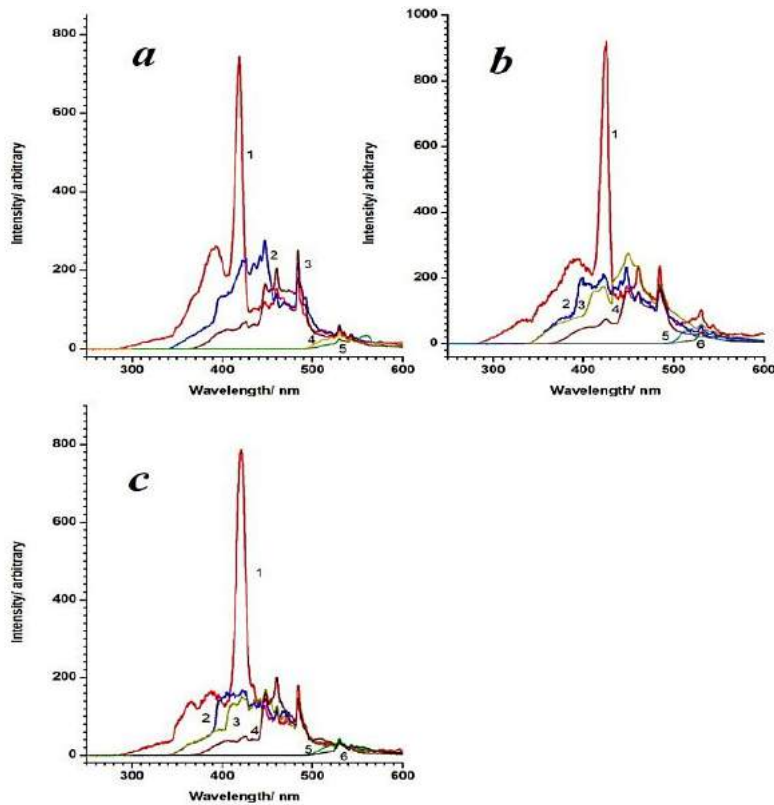


Fig. 5. Luminescence spectra:

- a. $\text{Bi}_{0.97}\text{Sb}_{0.03}$ at excitation from: 1- 237nm, 2- 285nm, 3 - 337nm, 4 - 377nm, 5 - 423nm;[3]
- b. $\text{Bi}_{0.88}\text{Sb}_{0.12}$ and c. $\text{Bi}_{0.85}\text{Sb}_{0.15}$ at excitation from: 1 -237nm, 2 -285nm, 3 -298nm, 4 337nm, 5 -377nm, 6 - 423nm.

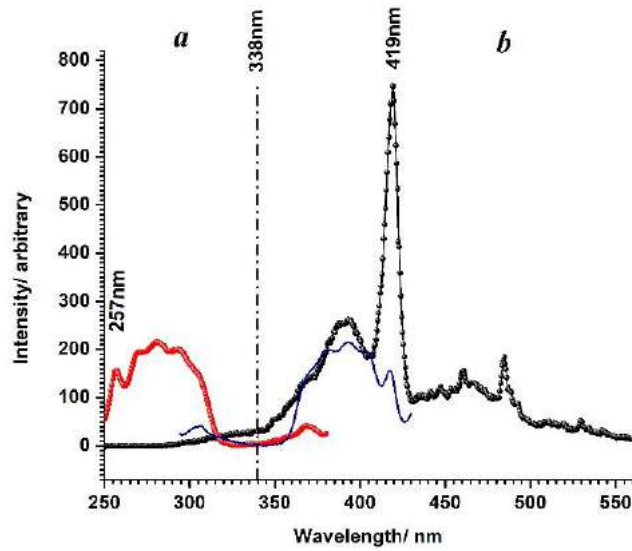


Fig. 6. Excitation spectra of (a) and luminescence (b) of $\text{Bi}_{0.97}\text{Sb}_{0.03}$ (semi-metallic state).

Table
Comparison of electronic transitions detected in the luminescence spectra of $\text{Bi}_{0.97}\text{Sb}_{0.03}$, $\text{Bi}_{0.88}\text{Sb}_{0.12}$ and $\text{Bi}_{0.85}\text{Sb}_{0.15}$ alloys at a temperature of 300 K in the range from 250 nm to 650 nm with theoretical calculations by the pseudopotential method [3].

Accounting		$\text{Bi}_{0.85}\text{Sb}_{0.15}$	$\text{Bi}_{0.88}\text{Sb}_{0.12}$	$\text{Bi}_{0.97}\text{Sb}_{0.03}$
[2]	[3]	624,6		
		603,7	606,2	
		587,7	597,2	
		571,9	571,7	573,2
		565,4		568,2
		553,7		558,2
		549		549,0
		543,3	543,9	542,7
		534,8		534,6
		530,2	530,8	530
		519,6	519,8	520,3
		512,6	513,5	513,6
498,6	496,6	503	502,3	
492,7		491,6	491,9	491,9
		484,7	485,3	485,4
		469,1	466,8	467,6
		460,9	460,9	460,9
		446,6	448,4	447,8
		439,4	442,2	435,8
		428,9	425,5	426
420,6		421,4	423,3	419,3
	417,8	410,6	408,5	409,3
		397,2	395,5	396
387,7	371,4	382,2	377,5	384,9
362,7	362,7	364,4	366,4	372,7
343,5	346,4	349,6	353,5	350,0
			334,5	332,6

[1] I.A. Bufetov and E.M. Dianov. Biopedoped fiber Lasers, Laser Physics Letters, vol. 6, issue 7, p.487-504, 2009.
 [2] B. Lenoir, M. Cassart, J. P. Michenaud, H.Scherrer and S. Scherrer. J. Phys. Chem. Solids, 1996, 57, 89.
 [3] S. Gölin. Band structure of bismuth:

Pseudopotential approach, Phys. Rev.,166, 643, 1968.
 [4] G. Blasse. Luminescence of Calcium Halophosphate $-\text{Sb}^{3+}$, Mn^{2+} at Low Temperatures. 1983, Chemical Physics Letters, vol. 104, pp.160-162.

- [5] *D.L. Dexter, C.C. Klick and G.A. Russell.* Criterion for the Occurrence of Luminescence. 1955, Physical Reviews, vol. 100, pp. 603-605
- [6] *P.Y. Wang, A.L. Jain.* Modulated piezo reflectance in bismuth, Phys. Rev., B2, 2978, 1970.
- [7] *A. West.* Chemistry of solids. Theory and applications. Moscow, "Mir", 1988.
- [8] *L.T. Butenko., S.M. Ryabikh, A.K. Bugayenko.* Vestnik MSU, Chemistry series, vol. 49, №6, 2008 (in Russian).
- [9] *P. Pelikán and M. Breza.* Classification of the possible symmetries of the Jahn-Teller systems, Chem. Papers 39 (2) 255-270,1985.
- [10] *I. Bersuker.* Yahn- Teller effect and vibronic interactions in modern chemistry, Moscow: Science, 1987.
- [11] *U. Opik.* Studies of the Jahn-Teller Effect. I. A Survey of the Static Problem, Proceedings of the Royal Society A: Mathematical, Physical and Engineering Sciences, 1957, vol. 238, № 1215, p. 425-447.
- [12] *I. Bersuker.* The Jahn-Teller Effect, Cambridge University Press, 2006, p. 632.
- [13] *A.B. Shick, J.B. Ketterson, D.L. Novikov, A.J. Freeman.* Phys. Rev. B, vol.60, №23, 1999, p. 15 484-15 487.

Received: 03.10.2019